Journal of Catalysis 270 (2010) 40–47

Contents lists available at ScienceDirect

Journal of Catalysis

journal homepage: www.elsevier.com/locate/jcat

Mechanism of dynamic structural reorganization in polyoxometalate catalysts

Hari Nair [a], Jeffrey T. Miller [b], Eric A. Stach [c], Chelsey D. Baertsch [a,*]

[a] School of Chemical Engineering and Birck Nanotechnology Center, Purdue University, 480 Stadium Mall Drive, West Lafayette, IN 47907, USA
[b] Argonne National Laboratory, CSE, 9700 S. Cass Ave., Argonne, IL 60439, USA
[c] School of Materials Engineering and Birck Nanotechnology Center, Purdue University, 1205 W. State St., West Lafayette, IN 47907, USA

ARTICLE INFO

Article history:
Received 29 September 2009
Revised 1 December 2009
Accepted 5 December 2009
Available online 20 January 2010

Keywords:
Phosphomolybdic acid
MPA
Isobutane oxidation
Twinning
Catalyst reconstruction
Catalyst activation
Thermal degradation
High resolution transmission electron microscopy

ABSTRACT

Understanding the structural and electronic mechanisms by which catalysts activate and deactivate during use is crucial to the intelligent design of more efficient chemical syntheses. Atomic resolution electron microscopy is used in conjunction with bulk characterization tools including as X-ray Diffraction (XRD), Ultraviolet–visible Diffuse Reflectance Spectroscopy (UV–vis DRS) and X-ray Absorption Spectroscopy (XAS) to understand the activation and deactivation mechanism of dodecamolybdophosphoric acid (MPA), a promising parent material for a class of polyoxometalate catalysts useful for the direct oxidation of isobutene to methacrylic acid. These techniques show that the thermal and reactive reconstruction of MPA arises from the migration of an oxomolybdate species from the cubic form of the anhydrous MPA structure. The reconstruction continues and results in complete degradation to MoO_3, which is inactive for isobutane oxidation. The mechanism by which reorganization occurs is investigated using High Resolution Transmission Electron Microscopy (HR-TEM) for the first time. These HR-TEM studies provide a picture of the atomic-scale rearrangement occurring in the catalyst. The initial structural reorganization in MPA is observed as the formation of annealing twins in the cubic form of the anhydrous polyoxometalate – this twinned structure is believed to be the active form of the catalyst. This twinning phenomenon is believed to originate from vacancies created in the MPA structure by the migration of atoms out of the primary structure. The twins then propagate across the MPA crystal and result in complete degradation of the MPA to MoO_3.

1. Introduction

Methacrylic acid is a commercially important organic intermediate with worldwide production of over 14 billion kilograms annually [1]. Currently, the most common approach for methacrylic acid synthesis is the hydrolysis of methacrylamide sulfate, obtained from acetone cyanohydrin, which in turn is produced through the reaction of acetone and hydrogen cyanide. In addition to its inherent safety concerns, this process produces inorganic byproducts that are difficult to dispose. An alternative process that is simpler, cleaner and safer is the oxidation of isobutane to methacrylic acid. The Keggin form of polyoxometalates such as dodecamolybdophosphoric acid (MPA) and its derivatives are widely acknowledged to be active and selective catalysts for the production of methacrylic acid by this route [2–9]. However, performance issues limit the commercial use of MPA and its derivatives. It has been shown that the native form of MPA and its derivatives are not catalytically active themselves, but rather, active catalyst structures evolve during reaction [9–13] – this creates an activation period during which the product yield of the catalyst is low. The structural modifications required for activation subsequently lead to degradation of the active form into an irreversible inactive form, limiting the lifetime of these catalysts.

While a number of studies have focused on the different forms of MPA during the activation and subsequent deactivation using bulk-scale characterization techniques, a detailed understanding of the mechanism of structural modification is not available, yet such detail is critical for formulating techniques to preserve the active form. The work presented here uses a combination of X-ray Diffraction (XRD), Ultraviolet–visible Diffuse Reflectance Spectroscopy (UV–vis DRS) and X-ray Absorption Spectroscopy (XAS) to observe bulk-scale structural transformations in MPA during heating. These techniques are used during thermal treatment and before and after isobutane oxidation reactions to show that the "activation" process in these catalysts occurs through the expulsion of Mo–O moieties out of the primary structure; structural changes initiated by this activation subsequently causes transformation to catalytically inactive MoO_3. High resolution transmission electron microscopy (HR-TEM) images show that the initial catalyst activation through the formation of annealing twins in the cubic form of the anhydrous polyoxometalate – this twinned structure is believed to be the active form of the catalyst. Subsequent propagation of the twins results in complete degradation of the MPA to MoO_3.

* Corresponding author. Fax: +1 765 494 0805.
E-mail address: baertsch@purdue.edu (C.D. Baertsch).

0021-9517/$ - see front matter © 2009 Elsevier Inc. All rights reserved.
doi:10.1016/j.jcat.2009.12.007

These mechanistic insights into the reconstruction process provide a rational basis for catalyst improvements that would enable the commercial use of polyoxometalate catalysts. Smaller activation times can be obtained by modifications that result in faster nucleation of the twins, and longer catalyst lifetimes can be achieved by utilizing structures that have more stability associated with the twinned structure or by suppressing twin propagation in the active phase. We also show how this mechanism accounts for the improved catalytic performance of vanadium-substituted MPA.

2. Experimental methods

2.1. Sample preparation

Commercially available dodecamolybdophosphoric acid (Nippon Chemicals) was dissolved in water to 0.01 M and dried at 293–773 K.

2.2. Transmission electron microscopy

Transmission electron micrographs were collected on a FEI Titan 80/300 field-emission environmental cell transmission electron microscope. HR-TEM samples were prepared by depositing a 0.01 M aqueous solution of MPA on a carbon grid and drying at 400 K. HR-TEM images were simulated for all known structures of MPA using a commercially available MacTempas TEM image simulation package. Samples were studied at different accelerating voltages and for different lengths of time to ensure that beam damage was not responsible for any observed structural changes.

2.3. Isobutane oxidation reactions

Reactions were carried out at steady state in a continuous flow, vertical U-tube quartz reactor. The reactor was fixed in a furnace with temperature controlled through a thermocouple placed in a dimple approximately 2 mm above the center of the catalyst bed. Catalysts were sieved to 125–250 μm particles, and 0.05–0.1 g was dispersed on the reactor bed. All samples were pretreated in simulated air (22% O_2/Bal He) for 1 h at reaction temperature. Reactant and product concentrations were measured using an Agilent 6890GC with FID and TCD detection (HP-PLOT Q column).

2.4. X-ray Diffraction

X-ray powder diffraction (XRD) patterns were recorded using a Scintag X2 Powder Diffractometer with Cu Kα radiation and a scanning rate of 1 deg/min.

2.5. Ultraviolet–visible Diffuse Reflectance Spectroscopy

Ultraviolet–visible (UV–vis) diffuse reflectance spectra (DRS) of prepared catalysts were obtained using a Varian (Cary 5000) spectrophotometer with a Harrick-Scientific Praying-Mantis diffuse reflectance accessory (DRA) and in situ cell (HVC-DRP). Data were collected by linear scanning in units of cm^{-1} over the range of 3500–50,000 cm^{-1}. All samples were ground before measurements, and magnesium oxide was used as reflectance reference. Reflectance measurements were converted into pseudo-absorbance units using the Kubelka–Munk transform [14].

2.6. X-ray Absorption Spectroscopy

Mo K edge EXAFS and XANES data were collected on the insertion-device beam line of the Materials Research Collaborative Access Team (MRCAT, Sector 10 ID) at the Advanced Photon Source, Argonne National Laboratory. A cryogenically cooled double-crystal Si (1 1 1) monochromator was used in conjunction with an uncoated glass mirror to minimize the presence of harmonics. The monochromator was scanned continuously during the measurements with data points integrated over 0.5 eV for 0.07 s per data point. Measurements were made in transmission mode with the ionization chambers optimized for the maximum current with linear response (~10^{10} photons detected s^{-1}) using a mixture of N_2 and He in the incident X-ray detector and a mixture of ca. 20% Ar in N_2 in the transmission X-ray detector. A Mo foil spectrum was acquired simultaneously with each measurement for energy calibration.

3. Results and discussion

The Keggin form of MPA has three levels of structure associated with it – primary, secondary and tertiary. The primary structure is the atomic arrangement (Fig. 1a) and consists of a central tetrahedron PO_4^- ion surrounded by 12 MoO_6 octahedra [15,16]. The secondary structure is the crystal structure, and different crystalline phases are known to exist depending on the extent of hydration [15,17–21]. Fig. 1b shows the cubic $H_3PMo_{12}O_{40}{\cdot}30H_2O$ structure viewed along the [1 1 0] direction. The secondary structure varies with the temperature of recrystallization and can be determined from XRD patterns (Fig. 1c). Recrystallization at room temperature results in a hydrated structure containing a mixture of $H_3PMo_{12}O_{40}{\cdot}30H_2O$ and $H_3PMo_{12}O_{40}{\cdot}13H_2O$. Treatment at 573 K for 1 h results in a mixture of anhydrous acid in a rhombohedral crystalline arrangement [17] and a cubic form, as reported by Wienold et al. [10]. Upon recrystallization from solution at 773 K or during heat treatment at 773 K, the XRD pattern changes dramat-

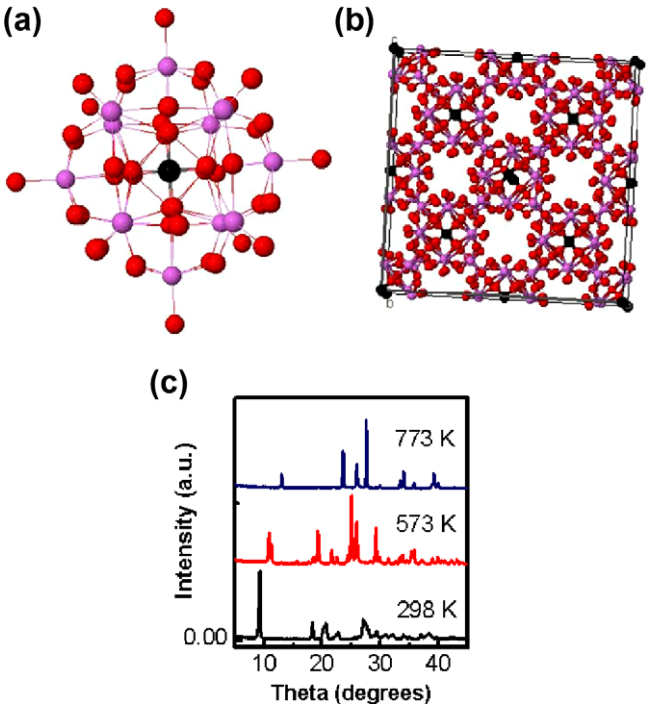

Fig. 1. (a) Primary or molecular structure of MPA ($H_3PMo_{12}O_{40}$) consisting of central PO_4^{3-} tetrahedron surrounded by 12 MoO_6 octahedra – red atoms correspond to O atoms, violet atoms correspond to Mo atoms and black atoms correspond to P atoms. (b) Secondary or crystalline structure of MPA (based on Allman [21] for $H_3PMo_{12}O_{40}{\cdot}30H_2O$) – same atom colors as (a). (c) XRD patterns collected over MPA samples recrystallized or heat treated at 298 K, 573 K and 773 K for 90 min. (For interpretation of the references to color in this figure legend, the reader is referred to the web version of this article.)

ically and resembles that of orthorhombic MoO_3, indicating that complete decomposition of the MPA to MoO_3 occurs at high temperatures. The tertiary structure is found to be dependent on macroscale catalytic properties such as pore size and particle size of the bulk material.

A typical activation process for isobutane oxidation over MPA at 653 K is shown in Fig. 2a. The yield of methacrylic acid remains extremely small (~5% selectivity, <10% conversion) until about 80 h on stream (activation period), after which it increases (15–20% selectivity, ~20% conversion), as similarly shown in previous reports and patents [2–9]. In contrast, materials such as MoO_3 (Fig. 2b) are not active catalysts for this reaction. Though the conversion and selectivity obtained even after MPA activation are quite low, they can be increased substantially through the addition of additives. Previous studies [22] have indicated that the use of substituted MPA can further enhance its performance as a catalyst. Our studies on $H_{15-x}[PMo_xV_{12-x}O_{40}]$, $6 < x < 12$ (Fig. 2c) show that substituting some of the Mo atoms in the primary structure considerably shortens the activation time (20 h vs. 80 h) and increases methacrylic acid yield. This improvement in catalyst performance has generally been attributed to the faster ejection of the V atoms from the primary structure in comparison with Mo atoms in the native MPA structure; however, there is no clear understanding of exactly why this should affect the catalyst performance. Other additives such as Cs, Fe, pyridine and niobium [6,7,23,24] have been found to increase the lifetime of the active form of the catalyst and improve methacrylic acid yields.

In this study, it was chosen to study the parent MPA form of the polyoxometalate as a base case, since the activation process is the same for the derivatives; the homogenous MPA structure allows for more ease of TEM analysis. While MPA is not necessarily the most viable catalyst for the production of methacrylic acid, its characterization provides the most understanding of how these catalysts activate and deactivate and how they can be changed to improve their performance. Based on the XRD pattern in Fig. 1c, it is expected that the anhydrous MPA structures would be precursors to the active form of the catalyst during reaction at 653 K, most likely in the cubic form as has been previously suggested [10].

Effects of thermal treatment on the electronic and geometric structure changes were studied using UV–vis DRS and XAS. UV–vis absorption spectra collected on the MPA catalyst at various times during thermal treatment at 773 K are shown in Fig. 3a. The initial MPA structure shows a single absorption edge at ~2.3 eV, characteristic of O–2p → Mo–d electronic excitations and is consistent with previous reports [25,26]. At the initiation of thermal treatment at 773 K, a shift in the absorption edge towards higher energies is observed. After about 20 min of treatment, the sample shows only one absorption edge at 2.97 eV, which is characteristic of MoO_3 [27]. The variation in the absorption edges suggests a transition to bulk oxide through the formation of intermediate structures, possibly due to the migration of oxometalate species from inside the primary structure (which later condense to form MoO_3). During this decomposition, only one absorption peak is seen, which suggests that no significant amount of MoO_3 is produced until the end of the reorganization process; based on our previous studies, [27] if this was not the case, a second absorption peak would begin to emerge at ~2.97 eV corresponding to the appearance of bulk MoO_3. Additionally, an absorption peak develops at ~1.3–1.4 eV, characteristic of d–d electronic transitions in metal oxides, indicative of a reduction process resultant from or causing the structural reorganization at elevated temperatures. Fig. 3b shows the UV–vis absorption spectrum of a catalytically active MPA sample – the catalyst was activated during isobutane oxidation at 653 K and then cooled in the reaction atmosphere before transferring the sample into the spectrophotometer. While the fresh catalyst shows a single edge at 2.3 eV, the catalytically activated sample shows two absorption

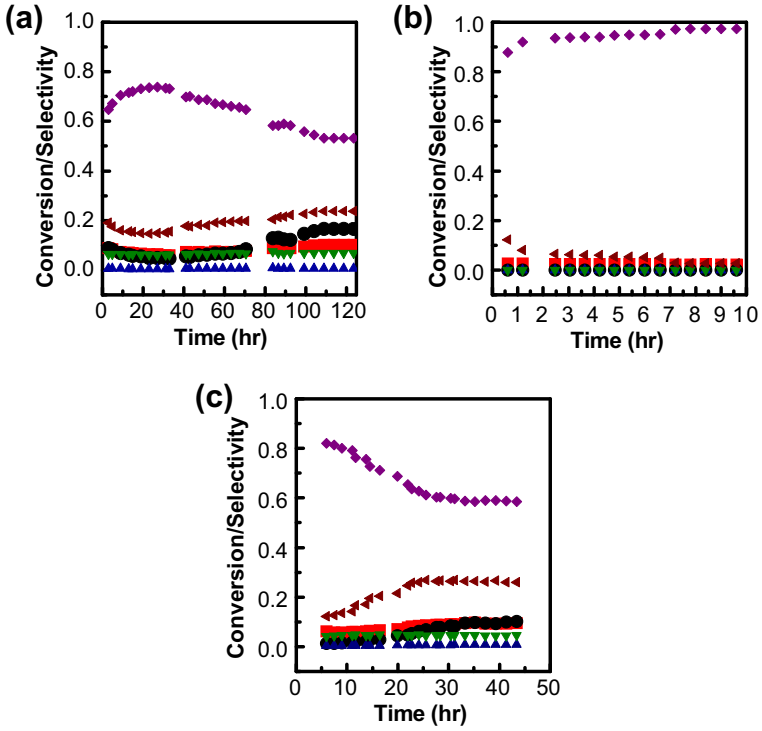

Fig. 2. Isobutane conversion and selectivity to different products as a function of time over (a) MPA (activation of MPA ~ 80 h), (b) MoO_3 (no methacrylic acid is produced even after ~50 h of reaction) and (c) $H_{15-x}[PMo_xV_{12-x}O_{40}]$, $6 < x < 12$ (much shorter activation periods are observed). Isobutane Conversion (■) Methacrylic Acid Selectivity (●) Methacrolein Selectivity (▲) Acetic Acid Selectivity (▼) Carbon Monoxide Selectivity (◆) Carbon Dioxide Selectivity (◀). (For interpretation of the references to color in this figure legend, the reader is referred to the web version of this article.)

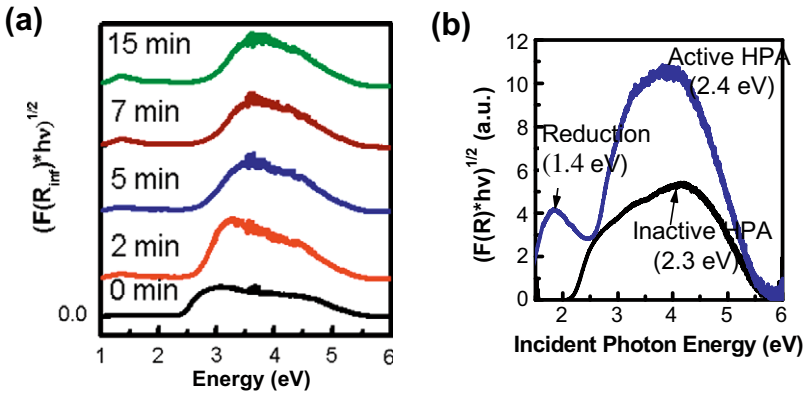

Fig. 3. (a) UV–vis absorption spectra during heat treatment of MPA at 773 K. (b) UV–vis absorption spectra for unmodified (inactive) $H_3PMo_{11}VO_{40}$ and activated $H_3PMo_{11}VO_{40}$ – activation was carried out by isobutane oxidation at 653 K.

edges at ~2.7 eV and 1.4 eV – clear reduction of the catalyst is observed during activation, and this spectrum suggests a structure identical to intermediate observations during the thermal treatment studies. It should be noted that UV–vis absorption spectroscopy is a bulk technique, and the analysis presented here does not include a quantitative measure of the fraction of Mo atoms that are reduced during the activation. The reduction of the metal atom has previously been shown to be important for the activation of the polyoxometalate structure and is also a major reason most reactions are carried out under reducing conditions [2,6,11,12,23,24,28,29]. In particular, Davis and coworkers have shown that the reduction of Mo and V atoms in a vanadium-substituted polymolybdate structure through the addition of niobium and pyridine leads to a more active and selective catalyst for the oxidation of *n*-butane [23,24].

As is evident from the UV–vis absorption studies presented here and from previous work, the activation process is associated with structural changes and these structural changes match with those that occur during thermal treatment – in fact, thermal stability is known to be extremely important for catalyst stability [30,31]. Wienold et al. have used a combination of X-ray Diffraction and X-ray Absorption Spectroscopy to show that the structural evolution of MPA during thermal treatment under reactive and non-reactive conditions occurs through the ejection of Mo atoms and the formation of a lacunary structure [10]. Structural investigations in this work using UV–vis DRS confirm that the activated bulk structure matches with intermediate structures obtained during the thermal reconstruction of MPA by treatment at 773 K and is similar to those reports mentioned earlier. Because the structural transformations are the same in both cases and the time period characteristic of structural changes at elevated temperatures is significantly shorter than that required for structural rearrangement under reaction conditions, all further investigations reported here utilized thermal decomposition to probe structure reorganization mechanisms during activation/deactivation mechanisms by simply heating and holding the catalyst at 773 K.

Changes in the primary structure were further inferred from XAS. X-ray absorption near-edge spectra (XANES) obtained at the Mo K edge for MPA during thermal treatment are shown in Fig. 4a. The intensity of the pre-edge feature (~20.005 keV) in the Mo K edge XANES has been shown to be a function of the extent of distortion of the octahedral coordination of the Mo atom – samples with distorted octahedral coordination (e.g. ammonium heptamolybdate) show higher intensity than those where the octahedral coordination is undistorted (e.g. MoO_3). As seen in Fig. 4a, the intensity of the pre-edge and hence the coordination of the Mo atom, which reflects the primary structure of MPA, remain unchanged on heating to 573 K. This corresponds to changes in the extent of hydration and is consistent with the XRD patterns reported above. At 573 K, the secondary structure is expected to be the anhydrous form, as determined from XRD, and is expected to be the precursor for the active catalyst at 653 K. Further heating to 773 K and subsequent treatment at that temperature lead to an increase in the intensity of the pre-edge feature, indicating that the primary structure is now modified, leading to a distortion in the Mo coordination. Further information about the local Mo environment is obtained from extended X-ray absorption fine structure (EXAFS) spectra collected at the Mo K edge. The magnitude of the Fourier Transform for the k^2-weighted spectra collected at the Mo K edge for MPA during heating to and when held at 773 K is shown in Fig. 4b. Two sets of peaks are observed in the spectrum obtained at room temperature. An inherent artifact of the data collections appears at ~1.2 Å. Peaks at smaller distances (~1.6 Å) correspond to scattering from O atoms immediately adjacent to the Mo, and peaks at larger distances (~3 Å) correspond to Mo, O and P atoms at larger distances [10]. A decrease in the intensity of peaks associated with scattering from further neighbors and a simultaneous change in the intensity of the peak due to the nearest neighbors is observed. These changes are similar to those observed by Ressler and coworkers, who fitted this data and concluded that there was a increase in the Mo–O bond distances during activation [10]. Due to these changes, the spectrum for the catalyst during treatment at 773 K resembles that obtained for ammonium heptamolybdate (AHM), which has a highly disordered structure compared to MPA. The imaginary part of the k^2-weighted EXAFS spectra of MPA after thermal treatment for 1 h matches with that observed for MoO_3 (Fig. 4c), confirming that the final structure formed during decomposition is a polyoxometalate species similar to MoO_3. Wienold et al. [10] have previously observed similar changes in EXAFS spectra collected from MPA during propene oxidation at various temperatures. Since the spectra shown here indicate the same changes as reported previously, a detailed fitting of the various bond lengths was not performed. Based on the results of Wienold and coworkers, it is, however, clear that (a) the structure at reaction temperature (653 K) is the cubic form of MPA, which is exactly what is expected from the XRD results presented above and that (b) the degradation results in the migration of a metal oxide entity from inside the structure to outside the primary structure, i.e. formation of a lacunary structure. The final XAS spectrum after thermal decomposition matches that observed in the Wienold study as orthorhombic MoO_3. Thus, XRD, UV–vis DRS and EXAFS analysis on the MPA during degradation points to the formation of an activated lacunary structure and a bulk oxide species formed by polymerization of oxides ejected from the primary structure of the MPA – a

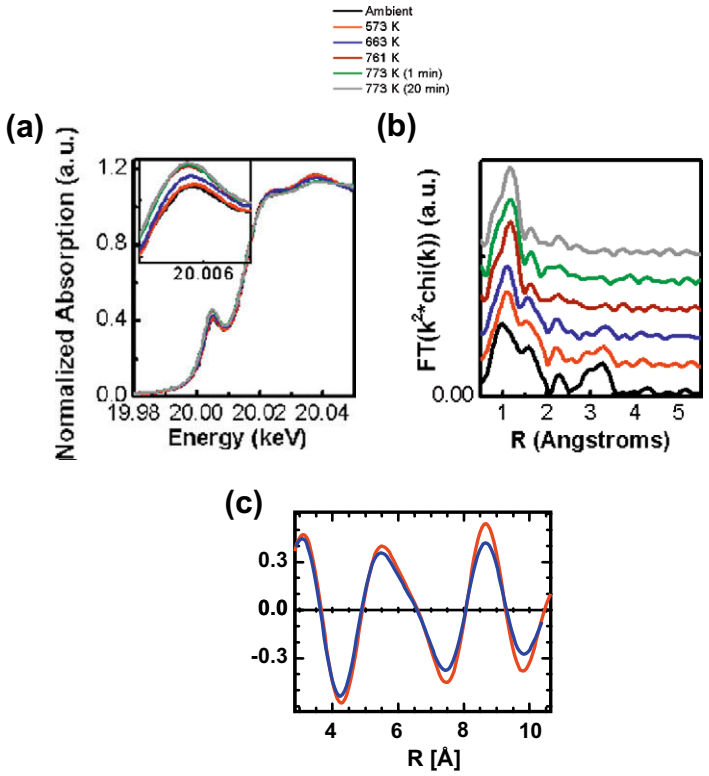

Fig. 4. (a) XANES spectra collected at the Mo K edge for MPA during heating to 773 K and held at 773 K as a function of time. (b) Magnitude of the Fourier Transform of the spectra collected at the Mo K edge for MPA during thermal treatment. (c) Imaginary part of the Fourier Transform of the k^2-weighted spectrum obtained for Mo HPA after thermal treatment (red) and for MoO_3 (blue).

picture that agrees with previous reports based on EXAFS and NMR studies [10,13,22,30–32]. As mentioned earlier, reaction studies have shown that MoO_3 is completely inactive for methacrylic acid production (Fig. 2b), verifying that the activated catalyst is the lacunary Keggin structure and not the metal oxide structures formed during decomposition.

The combination of these bulk techniques gives an idea of the average electronic/structural changes occurring during the activation/decomposition process. However, no specific information is available on the mode of structural reorganization, yet such information is essential to propose methods to improve the catalyst performance. To understand this mechanism, the degradation of MPA was studied at the atomic scale using a FEI Titan 80/300 field-emission environmental cell transmission electron microscope. HR-TEM samples were prepared by depositing a 0.01 M aqueous solution of MPA on a carbon grid and drying at 400 K. Due to the complex structure of these catalysts in comparison with simpler metal catalysts usually studied using TEM, interpretation of these HR-TEM images requires correlation with image simulation approaches. HR-TEM images were simulated for all known structures of MPA over a range of sample thicknesses and defoci conditions [33,34]. Comparison of the simulated phase-contrast image (Fig. 5a overlay over actual image) with the obtained images (Fig. 5a) and diffraction patterns for the actual (Fig. 5c) and simulated structure (Fig. 5d) shows that the structure observed in the TEM is the anhydrous cubic form ($p\bar{n}3m$ symmetry, $a = 11.853$ Å) observed along the [1 1 0] direction (Fig. 5b). While this structure is expected to be prevalent at higher temperatures (>573 K) based on the other spectroscopic techniques, and hence is expected to be the precursor to the active catalyst, it is perhaps stabilized by the low pressure conditions ($\sim 10^{-7}$ torr) in the TEM. Further examination indicates that the bright spherical spots observed in the phase-contrast image correspond to Mo atoms in the crystal lattice when viewed in projection along the [1 1 0] direction – the outline of spherical spots in the image can be matched to a similar pattern correlated with the Mo atoms in the unit cell (outlined in yellow in Fig. 5a and b, respectively). Similar matching was also performed for images collected over other regions of the sample – it is thus clear that the initial structure is consistent with both XRD and XAS results presented above. Additionally, no changes were observed due to beam exposure – the initial cubic structure is thus completely stable, and any changes shown below are due to thermal treatment alone.

The MPA samples were then subjected to heating inside the TEM, and images were collected using a highly sensitive, high-frame rate digital camera (Tietz FX114). Images were recorded during sample heating and also time resolved at 773 K. Varying heating rates were used, and it was found that similar phenomena occurred in all cases. Phase-contrast images collected on a sample at 773 K and held at constant temperature are shown in Fig. 6a–c. In these figures, the presence of annealing or transformation twins is clearly seen; the lattice shows mirror symmetry across the boundary outlined in Fig. 6a [33] (twinning plane). This can be confirmed from the Fast Fourier Transform of the deformed structure (Fig. 6d). It is seen that the diffractogram spots corresponding to the $[1\,\bar{1}\,1]$ planes are elongated, indicating that the twinning plane corresponds to the $[1\,\bar{1}\,1]$ plane of the crystal and rotation of the crystal occurs through 180° (into the plane of the paper) on either side of this plane. This can be confirmed by creating a MPA crystal wherein part of the crystal is rotated through 180° around the $[1\,\bar{1}\,1]$ plane (Fig. 6e – the section of the crystal in the black rectangle has been rotated) and used as input for simulated TEM images for this structure. The simulated image (Fig. 6f) matches with the experimental images during thermal treatment, confirming that twinning through rotation about the $[1\,\bar{1}\,1]$ plane is occurring. It is also observed that the twin boundary propagates across the crys-

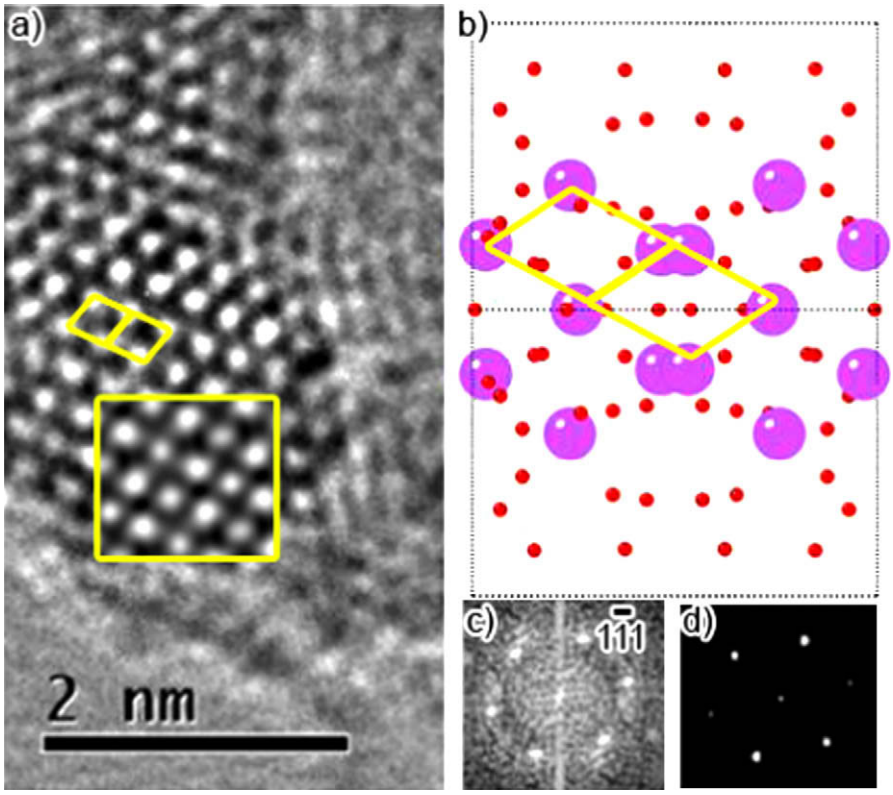

Fig. 5. (a) Phase-contrast electron micrograph obtained for recrystallized MPA on a C film. The overlay shows a simulated image obtained for the cubic form of the anhydrous acid [10], which is shown in (b) viewed along the 110 direction – red atoms correspond to O atoms, violet atoms correspond to Mo atoms and black atoms correspond to P atoms. The bright spots in the experimental image in (a), outlined by the yellow rectangle, correspond to the position of the Mo atoms in (b), outlined by the yellow rectangle. (c) Shows the Fast Fourier Transform (FFT) of the experimental phase-contrast image and (d) shows the simulated phase-contrast image. Diffraction spots are mapped in the FFT of the actual image. (For interpretation of the references to color in this figure legend, the reader is referred to the web version of this article.)

tal surface as the decomposition occurs (see Supplementary Movie S1). The time scale for this twinning process is on the order of minutes, which is consistent with the time scale associated with the reorganization observed using bulk-scale structure characterization techniques. Additionally, this twinning is found to occur in multiple places in the sample. The final structure obtained during decomposition in the TEM is a highly crystalline bulk structure (Fig. 6g) whose FFT matches with that obtained for MoO_3. The initial MPA structure shows an electron energy loss (EEL) spectrum with the Mo–$M_{4,5}$ absorption edge at 227 eV (Fig. 6h). The shape of the edge is characteristic of the local environment seen by Mo in MPA and changes drastically after heating. Comparison of the EELS spectrum collected after the decomposition process with that obtained for MoO_3 (Fig. 6h) confirms that the local structure seen by Mo in the completely decomposed sample is the same as in MoO_3. It is, therefore, clear that the decomposition process observed in the TEM is identical to that observed by the other characterization techniques.

The twinning deformation and its propagation shown in our HR-TEM studies are clearly critical to the structural reorganization of the MPA structure. However, without simultaneous monitoring of the catalytic activity, it is not possible to pinpoint whether the twinning is responsible for the activation process or the subsequent deactivation. The long-time scales and issues such as sample drift at higher temperatures required for activation under reaction conditions make this kind of in situ study infeasible. The similarity of the surface before and after twinning and the fact that it occurs on the cubic form of the MPA – which is the precursor to the active catalyst during reaction – suggests that the twinning phenomenon is more likely to be associated with the activation process. It is hypothesized that the vacancies created by the migration of Mo atoms to outside the primary structure provide nucleation sites (as seen in XAS) for the twinning to begin, resulting in the activation of the entire structure. Fig. 6e was simulated by removing Mo atoms at the interface of the twin, i.e. at the plane at which the rotated structure and the initial structure joint. The resultant structure contains a variety of Mo atoms with Mo–O bond distances and Mo–O–Mo bond angles different from the initial form. Changes in the extent of twinning would thus result in a disorganized form consistent with the XAS spectrum shown previously. It is our hypothesis that this highly strained twinned structure forms the basis of active sites for the isobutane oxidation reaction.

Additionally, the stability of the twinned structure determines the lifetime of the catalyst. It is our belief that some of the improvement seen in the performance of MPA though the incorporation of different elements into the structure is because of their effect on the twinning process [6,7,11,28,34]. As has been mentioned earlier, studies on $H_{15-x}[PMo_xV_{12-x}O_{40}]$, $6 < x < 12$ [22] have shown that activation is accompanied by ejection of V from the primary structure. Based on our studies on the mechanism of MPA activation, the greater ease of V removal in $H_{15-x}[PMo_xV_{12-x}O_{40}]$, $6 < x < 12$ in comparison with Mo removal in $H_3PMo_{12}O_{40}$ would result in faster formation of transformation twins and hence faster activation, consistent with our reaction results (Fig. 2c). The addition of other additives (e.g. Cs) [9,11,31] has been shown to increase catalyst lifetime, and our results suggest that this may be due to the formation of an MPA structure that is either more robust to the presence of twinned planes and vacancies or one wherein the propagation of twins is inhibited. Direct correlation between comprehensive bulk characterization methods and real-time images of atomistic mechanisms such as these provide unprecedented insight into the activation and deactivation of complex cat-

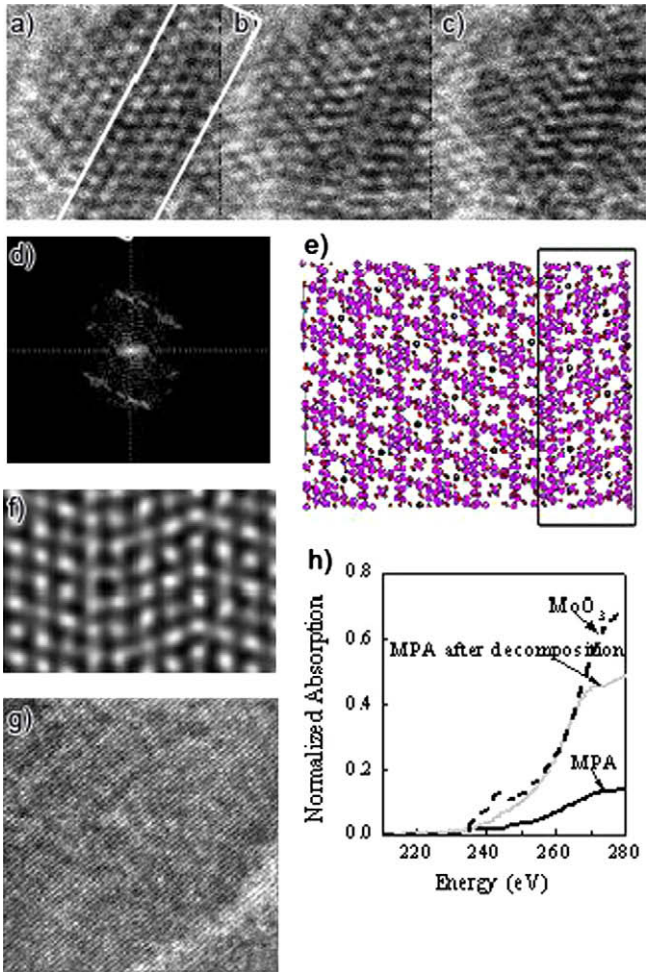

Fig. 6. (a–c) HR-TEM video-rate images obtained from MPA samples treated at 773 K in situ. (d) Diffractogram obtained from (a). (e) Crystal structure wherein part of the MPA crystal (outlined by black rectangle has been rotated by 180° around the $[1\,\bar{1}\,1]$ plane and (f) simulated image for the twinned structure shown in (e) – this matches with the zigzag patterns in (a–c). (g) Phase-contrast image of crystalline structure obtained after 20 min of treatment at 773 K and (h) EEL spectra collected from MPA, MPA after thermal treatment, and a reference spectrum from bulk MoO_3.

alysts and offer guidance for the synthesis of robust, efficient structures.

4. Conclusions

Structural transformations in dodecamolybdophosphoric acid (MPA) were investigated during thermal treatment as a method to understand transformations associated with the activation and deactivation of the catalyst during isobutane oxidation reactions. XRD, UV–vis DRS and XAS studies indicate that complete decomposition of catalytically inactive molybdenum oxide occurs on thermal treatment through the elimination of a Mo–O moiety from the primary structure. XRD studies show that the crystal structure of MPA changes with the extent of hydration of the crystal and that the precursor to the active catalytic form for isobutane oxidation at 653 K is most likely the cubic anhydrous structure. UV–vis DRS reveals that decomposition of the catalyst proceeds to MoO_3 and a reduction process is associated with this decomposition. X-ray absorption near-edge spectra indicate a transformation in the Mo atom coordination and along with EXAFS show the transition from the highly ordered MPA structure to a disordered structure akin to ammonium heptamolybdate, before decomposition to MoO_3. High resolution transmission electron microscopy was used for the first time to investigate these changes at the atomic level. Atomic resolution images of the MPA structure during the thermal treatment reveal that vacancies created due to ejection of the oxomolybdate species act as a nucleation site for the creation of annealing or transformation twins. The propagation of these twins results in complete decomposition of MoO_3, as also seen from other techniques. Manipulation of the properties of the materials affecting the rate of nucleation of the twins, and their propagations can lead to the development of highly active and stable MPA derivatives for the catalysis of isobutane oxidation.

Acknowledgments

H.N. is supported by the Bilsland Dissertation Fellowship at Purdue University and the American Chemical Society (PRF 48977-ND5). Synchrotron beam time was supported by Argonne National Labs GUP # 8603. The use of the Advanced Photon Source (APS) was supported by the US Department of Energy, Office of Science, Office of Basic Energy Sciences, under Contract No. DE-AC02-06CH11357. Materials Research Collaborative Access Team (MRCAT, Sector 10 ID) operations are supported by the Department of Energy and the MRCAT member institutions. The authors are extremely grateful to beamline scientists Soma Chattopadhyay and Tomohiro Shibata (MRCAT) for their assistance. TEM studies were carried out at the Birck Nanotecnology Center at Purdue University. The authors gratefully acknowledge Dr. Dmitri Zakharov, Dr. Seung-Min Kim and Mr. Robert Colby for their assistance.

Appendix A. Supplementary material

Supplementary data associated with this article can be found, in the online version, at doi:10.1016/j.jcat.2009.12.007.

References

[1] W. Bauer Jr., Ultmann's Encyclopedia of Industrial Chemistry, Wiley-VCH, Weinheim, 2002.
[2] M. Misono, Catal. Rev. 29 (2) (1987) 269–321.
[3] S. Yamamatsu, T. Yamaguchi, European Patent 425,666, Japan Patent 02,042,032, 1989.
[4] I. Matsuura, Y. Aoki, Japan Patent 05,331,085, 1996.
[5] K. Nagai, Y. Nagaoka, N. Ishii, European Patent 495-504-A2, 1992.
[6] N. Mizuno, M. Tateishi, M. Iwamoto, J. Catal. 163 (1) (1996) 87–94.
[7] N. Mizuno, M. Tateishi, M. Iwamoto, Appl. Catal. A – Gen. 128 (2) (1995).
[8] I.V. Kozhevnikov, Catalysts for Fine Chemical Synthesis: Catalysis by Polyoxometalates, vol. 2, John Wiley & Sons Ltd., West Sussex, England, 2002.
[9] M. Misono, Selective oxidation of butanes. Toward green/sustainable chemistry, Top. Catal. 21 (1) (2002) 89–96.
[10] J. Wienold, O. Timpe, T. Ressler, Chem. Eur. J. 9 (24) (2003) 6007–6017.
[11] F. Cavani, R. Mezzogori, A. Pigamo, F. Trifiro, E. Etienne, Catal. Today 71 (1–2) (2001) 97–110.
[12] F. Cavani, A. Tanguy, F. Trifiro, M. Koutrev, J. Catal. 174 (2) (1998) 231–241.
[13] C. Rocchiccioli-Deltcheff, M. Fournier, T. Faraday, J. Chem. Soc., Faraday Trans. 87 (1991) 3913–3920.
[14] P. Kubelka, F. Munk, Z. Tech. Phys. 12 (1931) 593.
[15] C.J. Clark, D. Hall, Acta Crystallogr. B 32 (5) (1976) 1545–1547.
[16] J.F. Keggin, Proc. Roy. Soc. Lond., Ser. A 144 (851) (1934) 75–100.
[17] L. Marosi, E.E. Platero, J. Cifre, C.O. Arean, J. Mater. Chem. 10 (8) (2000) 1949–1955.
[18] R. Strandberg, Acta Chem. Scand. Ser. A 29 (1975) 359–364.
[19] B. Herzog, W. Bensch, T. Ilkenhans, R. Schlogl, N. Deutsch, Catal. Lett. 20 (3) (1993) 203–219.
[20] H. d' Amour, R. Allman, Z. Kristallogr. 143 (1976) 1–13.
[21] R. Allmann, Acta Chem. Scand. Ser. A 29 (1975) 359–364.
[22] B.B. Bardin, R.J. Davis, Appl. Catal. A – Gen. 185 (1999) 283–292.
[23] M.E. Davis, C.J. Dillon, J.H. Holles, J. Labinger, Angew. Chem. Int. Ed. 41 (5) (2002) 858.
[24] C.J. Dillon, J.H. Holles, M.E. Davis, J.A. Labinger, Catal. Today 81 (2) (2003) 189.
[25] M.H. Youn, H. Kim, J.C. Jung, I.K. Song, K.P. Barteau, M.A. Barteau, J. Mol. Catal. A – Chem. 241 (1–2) (2005) 227–232.
[26] J. Melsheimer, S. Mahmoud, G. Mestl, R. Schlogl, Catal. Lett. 60 (3) (1999) 103–111.
[27] H. Nair, M.J. Liszka, J.E. Gatt, C.D. Baertsch, J. Phys. Chem. C 112 (5) (2008) 1612–1620.

[28] G. Busca, F. Cavani, E. Etienne, E. Finocchio, A. Galli, G. Selleri, F. Trifiro, J. Mol. Catal. A – Chem. 114 (1–3) (1996) 343–359.
[29] G. Mestl, T. Ilkenhans, D. Spielbauer, M. Dieterle, O. Timpe, J. Krohnert, F. Jentoft, H. Knozinger, R. Schlogl, Appl. Catal. A – Gen. 210 (1–2) (2001).
[30] T. Ressler, O. Timpe, F. Girgsdies, J. Wienold, T. Neisius, J. Catal. 231 (2) (2005) 279–291.
[31] M.J. Janik, B.B. Bardin, R.J. Davis, M.A. Neurock, J. Phys. Chem. B 110 (9) (2006) 4170–4178.
[32] J.W. Christian, The Theory of Transformations in Metals and Alloys, second ed., Pergamon, 2002.
[33] R. Kilas, MacTempas User Manual. Available from: <http://www.total.resolution.com/MacTempasManual.pdf>.
[34] T. Ilkenhans, B. Herzog, T. Braun, R. Schlogl, J. Catal. 153 (2) (1995) 275–292.